CFD STUDY OF FILTRATION PROCESS IN MOULDED FILTERS WITHIN A VACUUM PUMP

Nausheen Basha[a*], Lloyd Cochrane[b], Stacey Culham[b], Faik Hamad[a] and Zulfiqur Ali[a]
[a] Teesside University, Middlesbrough, UK
[b] PSI Global Limited, Stockton-on-Tees, UK

Abstract

Air/Oil filtration through filters is commonly utilised in the vacuum industry where oil lubricated pumps are used across a number of different applications such as food and packaging, industrial, pharmaceutical, R&D, forming and drying. The air/oil filters are crucial in the reduction of exhaust emissions, which, when suspended as fine particulate matter can cause great harm to the environment, climate, equipment life and public health. However, the behaviour of flow through the filters is not fully understood and much of the design and development work is based on historical know-how and experimental studies.

Computational Fluid Dynamics (CFD) is a powerful tool to understand the flow characteristics and droplet trajectory through the filters which is challenging through experimental techniques. In this study, a CFD model is developed by using the commercial ANSYS FLUENT code. Oil droplets from the pump entering the filter are treated as a discrete phase. Euler-Lagrangian frame is used to characterise the multiphase flow, K-Ɛ as a turbulence model, Rosin-Rammler distribution of oil droplets, User Defined Functions (UDF) are written for droplet injection, distribution and deposition. Various methodologies and tests were developed to obtain the required data to feed into the model and validate the data predicted by the computational model. The obtained computational data agrees well with the experimental data.

Keywords

Filtration, CFD, aerosol spectrometer, pressure drop, deposition.

1 Introduction

Filtration is one of the most common techniques used in Chemical/Process Engineering. It is used to separate solids from liquid, liquid from gas, liquid from liquid and vapour from gas. Filtration involves some form of media that would capture some form of a component in the mixture. Almost 80% of the pumps used today are lubricated with oil [1]. The filters when used in these pumps serve the purpose of cleaning the exhaust air from the pump, so that it is safe to release into the environment and the collected oil may be recovered for reuse or disposal. This study is focused on the filters that are manufactured by PSI Global Limited through a patented moulding process for application in a rotary vane vacuum pumps [2]. International occupational health and safety standards require that oil mist be reduced to 3 mg/m3 [3] . Therefore, it is important that the air from the vacuum pump when released to the atmosphere is free from any dispersed oil droplets

In spite of the popularity of the fibrous filtration technology in industrial application, relatively little is understood about the overall mechanism of the separation/filtration process. Pertaining to the complexity of the micro fibres, range of oil droplets generated and their deposition on the fibers, most of the studies relied on considering rather simple geometries solving analytical flow-field solutions. These geometries consisted of single fibres or regular arrays of a uniform arrangement of fibres assumed to be parallel, with flow perpendicular to the fibre axes. These studies highlighted the 2D representation of flow field across the fibres [4][5].

The flow through filters was traditionally studied for pleated filters. In 1990, Gurumoothy [6] modelled the flow across the whole of air induction system by applying an extended form of Darcy equation. His model had highly under-predicted the pressure drop when compared with the experimental data. Further models developed by Cai [7] and Tsang [8], for air intake filter predicted pressure drop close to experimental data. All the above studies considered the flow of solid particles dispersed in continuous air medium. Very little is understood on the flow of oil droplets. Recent studies with oil separation using fibrous filters have been segmented towards 3D micro-modelling. Here the mechanism of filtration such as interception, inertial impaction, diffusion, gravitational settling and electrostatic capture are included. Wang et al [9] , Maze et al [10] and Jaganathan et al [11] developed 3-D virtual fiber-web, made-up of infinity long fibers (spunbonded and electrospum filters), generated based on nonwovens characterization techniques for fibrous geometries [12], to simulate the filtration efficiency and pressure drop by solving the Navier-Stokes equations. Hajra et al. [13] optimised the fibre diameter for a better filter performance. Likewise, Hosseini and Tafreshi [14] presented a methodology for predicting the fibre drag and single filter efficiency during the particle loading process. Qian et al [15] used Stochastic algorithm and Discrete element method (DEM) to model and simulate the gas-solid flow characteristics in fibrous media exposed to particle loading which was validated by comparison with the empirical model from the literature. The influence of various

parameters including porosity, face velocity and particle size on the filtration performance of fibrous media had been investigated. Coupling of Lagrangian tracking and Volume-of-Fluid (VOF) solver provided a complete physics of droplet motion on fibres, it's coalescence and formation of liquid films which then breaks up under Plateau-Rayleigh instability [16]. Most of the available literature has been very popular with oil separation for compressed air application.

In this work, pressure drop is computed for a separator in a rotary vane vacuum pump application. This is done by varying the permeability and inertial resistance across the filter media due to the loading of oil droplets. Discrete Phase Model (DPM) is used to track the injected oil droplets through Rosin Rammler distribution and writing User Defined Functions (UDF) in FLUENT. The distribution of oil droplets at the pump's chamber/filter inlet is determined by Welas® Particle Counter along with a bespoke dilution chamber. Instantaneous pressure is computed for two different flow rates and the computed values are validated against the experimental data.

2 Numerical Formulation

2.1 Discrete Phase Model

In addition to solving the conservation equations for continuous medium i.e air, the discrete phase (oil droplets) are solved in a Lagrangian frame of reference. Through the Lagranian Frame Reference, the oil droplets can be tracked for their velocities and positions in the domain. Tracking every single aerosol is quite feasible in this scenario as the volume fraction of the discrete phase is 0.0001%.

2.1.1 Particle Transport Equation

FLUENT code predicts the trajectory of a discrete phase aerosol particle by integrating the force balance on the particle, which is based on the Lagrangian reference frame. The force balance of inertia force, drag force and gravitational force acting on the particle in the x direction can be written as [17].

$$\frac{du_p}{dt} = F_D(u - u_p) + g_x \frac{(\rho_p - \rho)}{\rho_p} + F_x \quad (1)$$

Where $F_D(u - u_p)$ is the drag per unit mass of the particle.

$$F_D = \frac{18\mu}{\rho_p d_p^2} \frac{C_D Re}{24} \quad (2)$$

Where, u is the air velocity, C_D the drag coefficient, u_p is the particle velocity, μ is the air viscosity, ρ is the air density, ρ_p is the particle density and d_p is the particle diameter, F_x is the additional forces than can be important under special circumstances such as virtual mass, Brownian force and lift force.

Figure 1 shows the path line of the particle, where it enters a cell and its track is modified within the cell after which it exits the cell while interacting with the continuous flow.

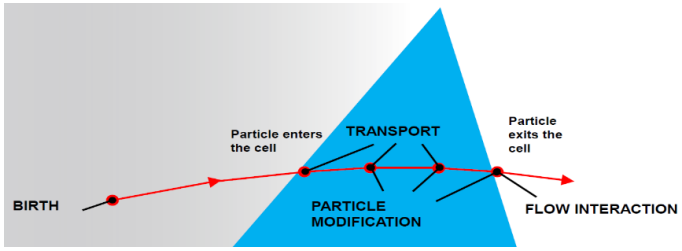

Figure 1: Particle Path Line

Particle positions are integrated for every ten time steps of the continuous flow and maximum number of steps to compute a trajectory is setup as 4000.

2.1.2 Particle Injection

The aerosol distribution at the upstream of the filter is measured using an Aerosol Spectrometer Welas®. This Spectrometer comes with a limitation on particle concentration. As a result, a dilution chamber is used along with it where a certain ratio of clean air is added. This ensures that the data collected is of good accuracy.

Figure 2 shows the typical location of the aerosol sampling probe in the pump and Figure 3 shows the aerosol distribution.

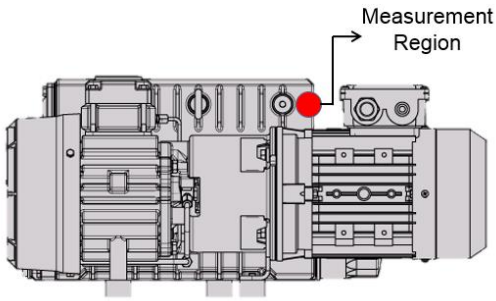

Figure 2. Upstream Measurement [18]

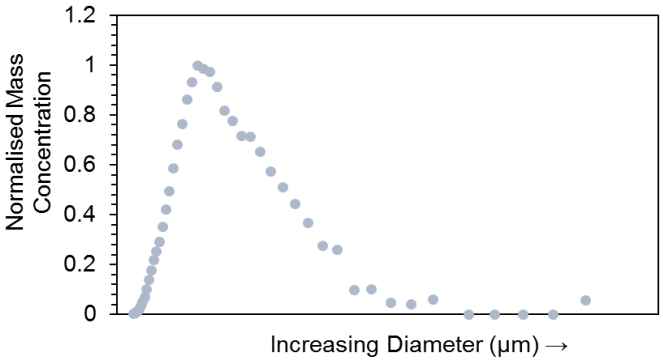

Figure 3. Aerosol Size Distribution at the Filter Inlet

The range of collected data is divided into discrete intervals representing a mean diameter for which the trajectory calculations will be performed. Due to a wide range of diameters, the injection type considered in this study is assumed that the droplet diameter distribution was based on Rosin-Rammler formulae. There is a reasonable correlation and the obtained experimental data matches very well with the Rosin-Rammler fitting.

2.2 Macroscale Modelling

The filter media is made up of glass fibres with small diameters in the micron range. Figure 5 shows an SEM image of the filter media with a magnification factor of 500.

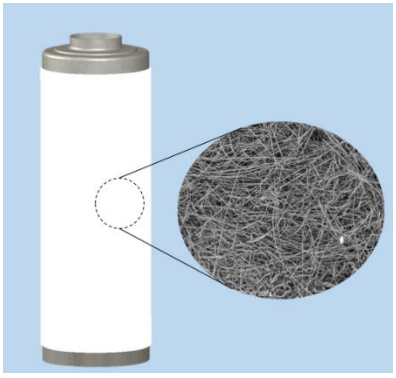

Figure 5: SEM Image of filter Media

This filter is modelled as 'Porous Zone' in ANSYS FLUENT, where the pressure drop is determined through the additional momentum source term along with the standard fluid flow equations.

For a homogeneous porous media, a standard source term can be expressed as,

$$S_i = -(\frac{\mu}{\alpha} v_i + C_2 \frac{1}{2} \rho v_{mag} v_i) \quad (3)$$

Where α is permeability, C_2 is the inertial resistance factor, ρ, μ and v are fluid density, viscosity and velocity. The first term on the right hand side of the equations represents viscous loss term and the second term represents inertial loss term.

User Defined Functions (UDF) are written to change the properties of porous media over time due to aerosol loading. With increasing time, the permeability increases in every cell of the porous zone. Therefore, for every time step, new values of inertial and viscous resistance are computed to account for the aerosol deposition in every cell.

2.3 Computation Domain and Boundary Condition

In this study, a filter with inner diameter D, outer diameter 1.5D and length 4.5D is considered. The filter is placed inside a chamber which is a part of vacuum pump (Figure 6). The filter media is a porous zone and the simulation is run under standard conditions.

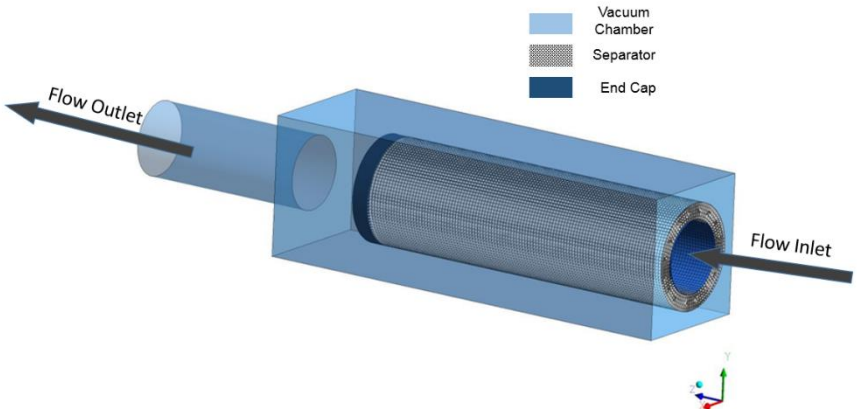

Figure 6. Computational Domain

3 Results and Discussion

3.1 Clean Air Flow

In the case of a clean air flow through the filter with the application of uniform resistances (inertial and viscous) in the x, y and z direction, there occurs a uniform variation in local pressure in the porous media. However, the regions circled in red shows a non-uniform distribution of pressure (Figure 7a). This is due to the fact that, at these regions there is a significant change in velocity gradient considering the boundary layer near the porous media and the endcap (Figure 7b). Therefore, the incoming flow towards the porous region of the separator has an effect on its pressure trend. There are higher chances that higher gradients would lead to uneven flow field in a filter, thereby uneven filtration.

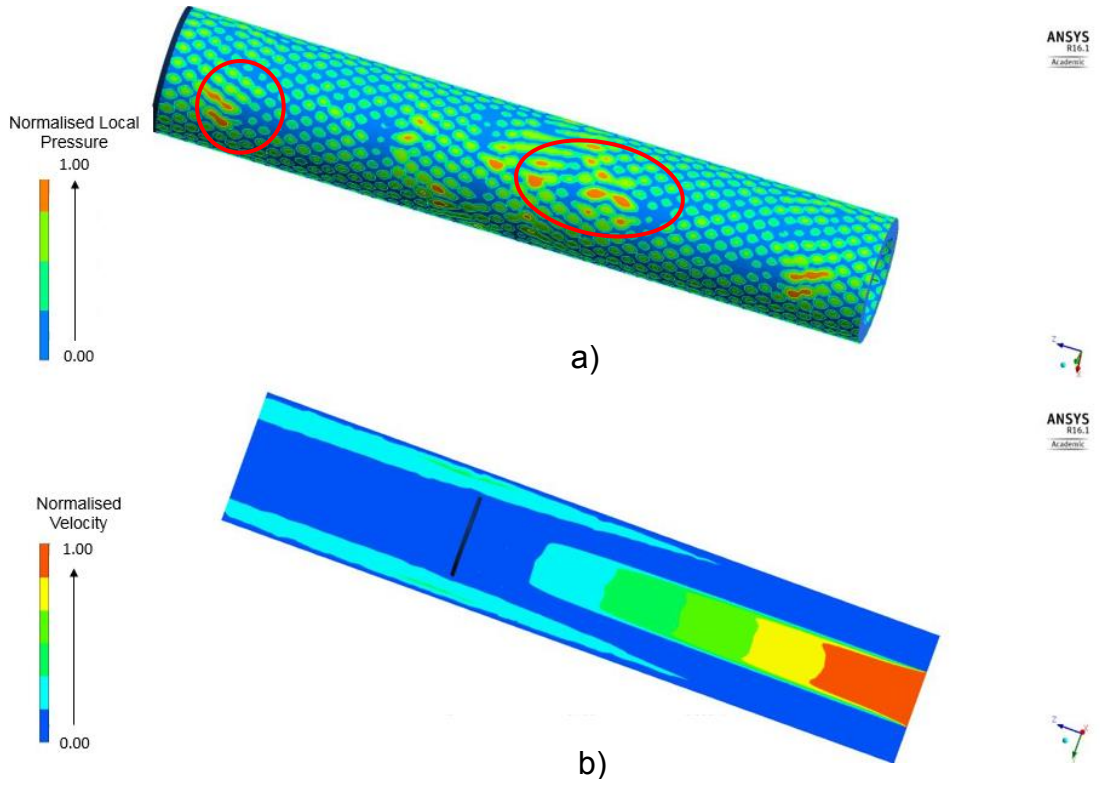

Figure 7. a) Local Pressure Contour b) Velocity Contour across Domain Cross Section

While considering the global pressure for a mid-section of the domain, it is seen that there is a linear change in pressure across Y axis of the filter represented in various coloured layers of the contour plot (Figure 8a).

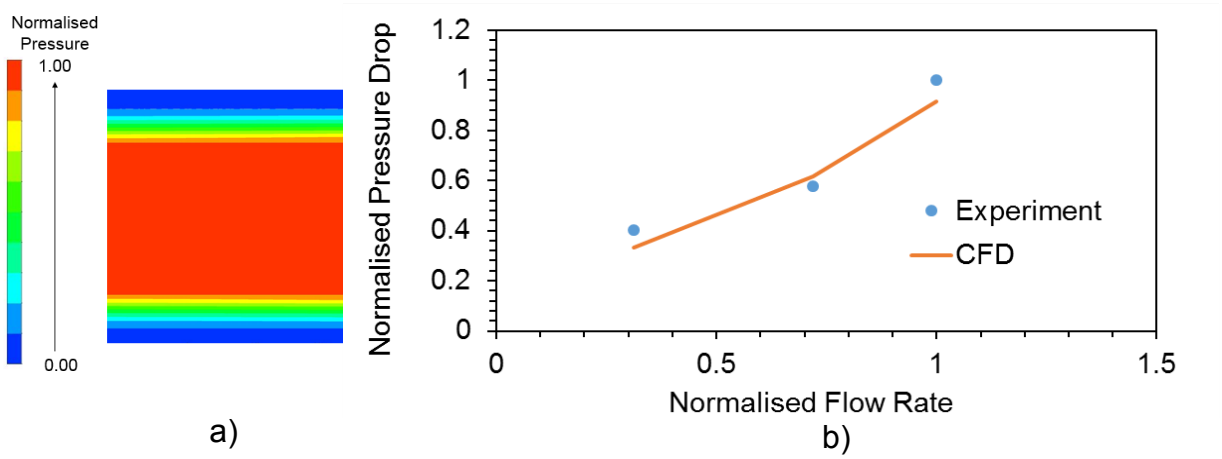

Figure 8. a) Pressure Distribution across Porous Media at 50% of Filter Length from Inlet, b) Data Validation

In order to validate, the data obtained through computation for the dry state is compared with the measured experimental values and this computational data stands out with the accuracy of 86% (Figure 8b). This gives the confidence that the calculated resistances can be carried forward for aerosol loading analysis.

3.2 Aerosol Loading

To simulate the aerosol loaded separators, oil droplets are allowed to deposit on the porous medium of the filter over time. Assuming all the dispersed oil droplets are

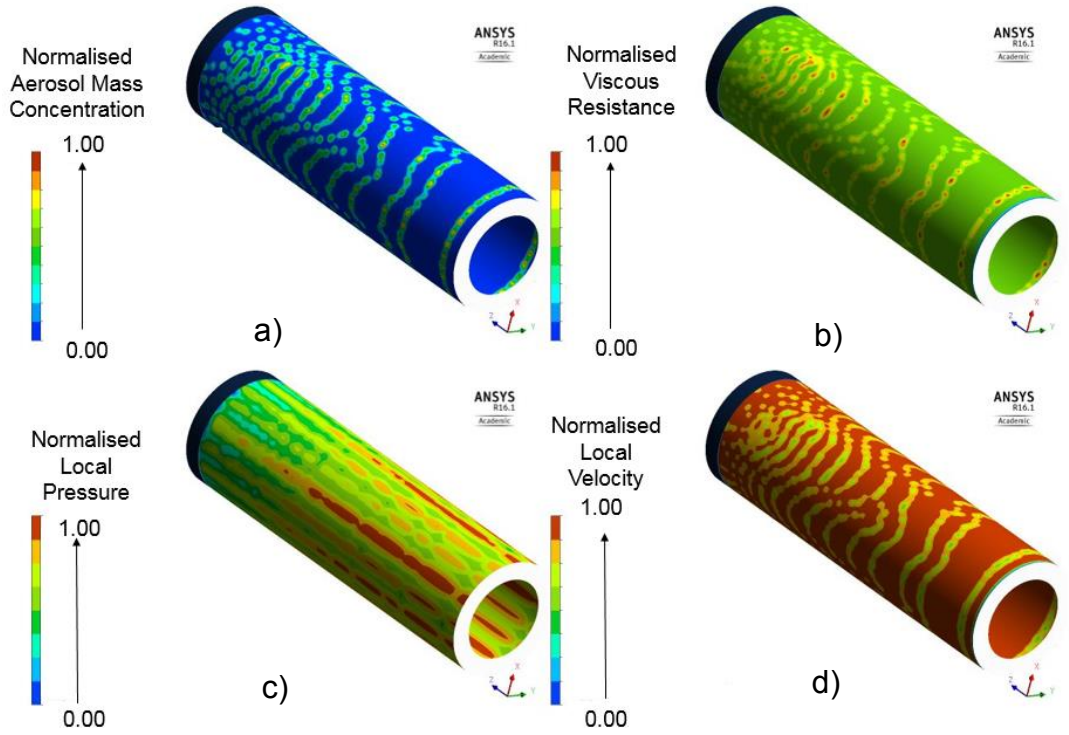

Figure 9. a) Contours of Aerosol Mass Concentration, b) Viscous Resistance, c) Pressure and d) Velocity on Porous Zone

collected by the filter, this forms numerous pockets of high and low mass concentration for the flow time of 30 minutes (Figure 9a). Particle streamlines tend to adjust their paths when they flow through the filter and the permeability is reduced or the viscous resistance is increased at those regions of deposition (Figure 9b). This as a whole affects the local pressure and velocity across the filter in comparison to the dry case, where the distribution is almost uniform (Figure 9c and 9d).

Comparing instantaneous aerosol loading for 5 minutes and repeating it for 30 minutes, it is very obvious that the aerosol loading increases with time. Normalised loading factor is chosen as a non-dimensional parameter for comparison, which is the ratio of mass concentration in the current cell to that of the maximum concentration within the domain. In addition to this, the contour plots for porous zone cut section show that the loading is at its least near the inlet, inconsistent at the mid-section and comparatively homogeneous near the end cap (Figure 10).

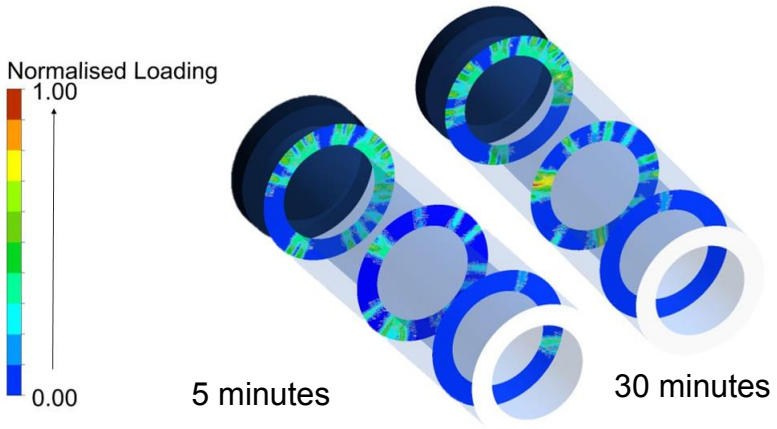

Figure 10. Normalised Loading Comparison for 5 and 30 minutes

Plotting the experimental and predicted data for single and two phase flow in Figure 11, it is clear that the slope of the curve is higher where there is higher loading. The

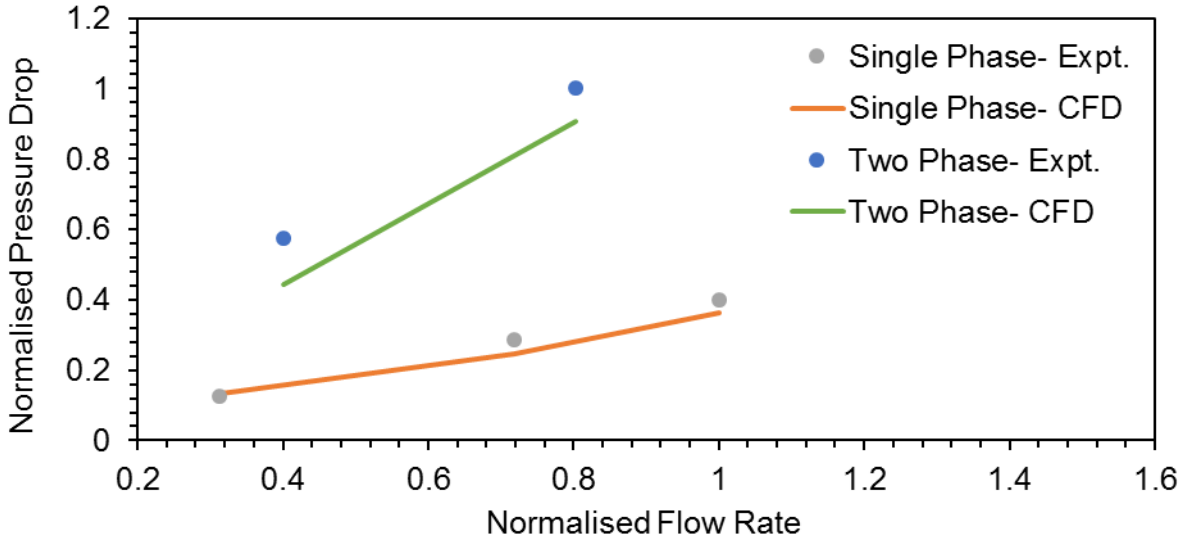

Figure 11. Data Validation

pressure drop across the filter changes with the mass of deposited aerosol droplets, this is due to the increase in resistance or lower permeability in comparison with the

single phase flow. For single phase flow the computational data agrees well with the experimental one with the accuracy of 90%. However, when the two phase is considered with the second phase being aerosol droplets this adds a level of complexity or additional terms to solve for in the fluid flow equations. Moreover, the oil droplets exibit the properties coalescing and drainage from the filter which need further work to include in the model. These add up to the average error percentage of almost 16.2%.

4 Conclusion

A CFD model was developed by using Euler-Lagrangian frame to investigate the oil–air flow in fibrous filter. The standard K-Ɛ turbulence model with standard wall function embedded in ANSYS FLUENT was used. User Defined Functions (UDF) are written for droplet injection, distribution and deposition. A number of test rigs were developed and built to obtain the required data to feed into the model and validate the data predicted by the computational model. The following conclusions can be drawn from the study:

- The Rosin-Rammler fitting applied to the experimental data using the values of minimum and maximum diameters fits very well with the experimental values which lead to selecting this option for droplet injection in discrete phase model.
- CFD with the UDF is an effective tool to study the aerosol loading mechanism over time
- The pressure drop data obtained from the model for droplet injection cases by considering the change in permeability and inertial resistance across the filter media by incorporating the UDF in model showed an increase with time. The data from the model are validated against experimental data for different flow rates. The preliminary results indicate the high accuracy and reliability of using the model to extrapolate the data for any flow rate conditions and for other filters.
- The experimentally validated model is used as a visual demonstration of 3-D distribution of mass concentration, velocity and pressure after the filter is used for 30 minutes in the vacuum pump.

References

[1] C. Rehman and H. Bloch, “Oil Mist-lubricated Pumps and Electric Motors,” Machinery Lubrication, Noria, 2006. [Online]. Available: http://www.machinerylubrication.com/Read/883/oil-mist-lubricated.

[2] D. M. Hunter, “Process and apparatus for moulding a filter,” WO/2011/010165, 2015.

[3] H. Senior and G. Evans, “Consultation on monitoring of water-miscible metalworking fluid (MWF) mists RR1044,” 2015.

[4] A. A. Kirsch and N. A. Fuchs, “Studies on fibrous aerosol filters. 3. Diffusional deposition of aerosols in fibrous filters.,” Ann. Occup. Hyg., vol. 11, no. 4, pp. 299–304, 1968.

[5] N. Rao and M. Faghri, “Computer Modeling of Aerosol Filtration by Fibrous Filters,” Aerosol Sci. Technol., vol. 8, no. 2, pp. 133–156, 1988.

[6] G. Vanchinath, “Computational fluid dynamics modeling of an air induction system,” University of Rhode Island, 1990.

[7] Q. Cai, “A Study of Air Filter Flow By Computational Fluid Dynamics,” Oklahoma State University, 1993.

[8] C. Tsang, “Analysis of pleated air filters using computational fluid dynamics,” 1997.

[9] Q. Wang, B. Maze, H. V. Tafreshi, and B. Pourdeyhimi, “Simulating through-plane permeability of fibrous materials with different fiber lengths,” Model. Simul. Mater. Sci. Eng., vol. 15, no. 8, pp. 855–868, Dec. 2007.

[10] B. Maze, H. Vahedi Tafreshi, Q. Wang, and B. Pourdeyhimi, “A simulation of unsteady-state filtration via nanofiber media at reduced operating pressures,” J. Aerosol Sci., vol. 38, no. 5, pp. 550–571, 2007.

[11] S. Jaganathan, H. Vahedi Tafreshi, and B. Pourdeyhimi, “Modeling liquid porosimetry in modeled and imaged 3-D fibrous microstructures,” J. Colloid Interface Sci., vol. 326, no. 1, pp. 166–175, 2008.

[12] B. Pourdeyhimi, R. Ramanathan, and R. Dent, “Measuring Fiber Orientation in Nonwovens Part I: Simulation,” Text. Res. J., vol. 66, no. 11, pp. 713–722, 1996.

[13] M. G. Hajra, K. Mehta, and G. G. Chase, “Effects of humidity, temperature, and nanofibers on drop coalescence in glass fiber media,” Sep. Purif. Technol., vol. 30, no. 1, pp. 79–88, 2003.

[14] S. A. Hosseini and H. Vahedi Tafreshi, “Modeling particle-loaded single fiber efficiency and fiber drag using ANSYS-Fluent CFD code,” Comput. Fluids, vol. 66, pp. 157–166, 2012.

[15] F. Qian, N. Huang, J. Lu, and Y. Han, “CFD–DEM simulation of the filtration performance for fibrous media based on the mimic structure,” Comput. Chem. Eng., vol. 71, pp. 478–488, 2014.

[16] R. Mead-hunter, “Modelling micro-scale coalescence and transport processes in liquid aerosol filtration,” 2012.

[17] I. Ansys, “ANSYS FLUENT theory guide,” Knowl. Creat. Diffus. Util., vol. 15317, pp. 724–746, 2009.

[18] Busch Vacuum Pumps and Systems, “R 5 RA 0025/0040 F.” [Online]. Available: http://www.buschvacuum.com/np/en/products/r+5/r%25E2%2580%25895%2Bra%2B0025%252F0040%2Bf.